Residual Motion Compensation in ECG-Gated Cardiac Vasculature Reconstruction

Chris Schwemmer, Christopher Rohkohl, Günter Lauritsch, Kerstin Müller and Joachim Hornegger

Abstract—Generating 3-D reconstructions of cardiac vasculature from angiographic C-arm CT (rotational angiography) data is a challenging problem. Currently, many approaches depend on a reconstruction from ECG-gated projection data either as a reference for further processing or as the final result. Due to imperfect gating, e.g. caused by irregular heart movement, residual motion corrupts these reconstructions.

We present an algorithm to compensate for this residual motion. The approach is based on a deformable 2-D–2-D registration between the acquired projection data and a forward projection of the initial ECG-gated reconstruction. It does not depend on an explicit segmentation of vasculature or markers, and works without user interaction. The estimated 2-D deformation field is compensated for in the backprojection step of a subsequent reconstruction. The algorithm is evaluated on two clinical datasets, showing a clear decrease in artefact level and better visibility of structure in the compensated reconstructions.

I. Introduction

A. Purpose of this Work

Three-dimensional information during cardiac interventions can provide improved guidance and easier assessment for complex interventional procedures [1], [2]. Ideally, this 3-D imaging should be performed in the interventional suite using C-arm CT, avoiding the need to move the patient to a CT scanner or perform a prior diagnostic CT scan. Additionally, up-to-date information of the current state would be available. Currently, this approach is limited by the temporal resolution of available C-arm systems. Due to the long acquisition time of several seconds, heart motion corrupts a straightforward 3-D reconstruction. This results in motion blur, streak artefacts and reduced sharpness and visibility of structure.

Commonly, an ECG signal is recorded during the acquisition. This allows to retrospectively gate the available X-ray projection data so that only images from a specific heart phase contribute to the 3-D reconstruction [3]. However, ECG data does not necessarily correspond to the exact motion state of the heart [3]. A wider gating window is desirable to get a high signal-to-noise ratio and little undersampling artefacts, but then the residual motion in the gated projection data needs to be compensated for.

B. State of the Art

In the literature, several approaches have been proposed to account for residual motion due to non-ideal ECG-gating. A
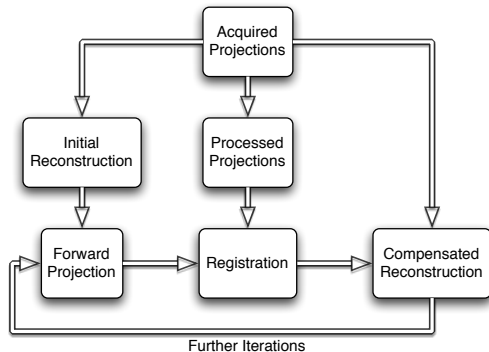
Figure 1: Illustration of the proposed algorithm.

full 3-D estimation is a strongly ill-posed problem with high computational demands. However, due to the ECG-gating, the residual motion inside one window can be assumed to be reasonably small and an approximate 2-D motion estimation in projection space might be sufficient. This is demonstrated both by previous work [4]–[6] and the results shown below.

A model-based learning approach was recently proposed, that registers a previously learnt motion model to the actual data [5]. Here, an extensive training phase is needed beforehand, and the application to patients with very irregular heart motion is difficult. A projection-based motion compensation was proposed in [6]. It requires a segmentation of vasculature centrelines in the acquired projection data, which is difficult [7].

C. Outline

In this paper, a method for compensation of residual motion in ECG-gated data is presented. Our method estimates residual motion by deformable 2-D–2-D registration in projection space without requiring complex image pre-processing steps.

In the next section, our algorithm and the experimental setup is discussed in detail. In Section III, the results are presented and both a qualitative and quantitative evaluation is performed.

II. Materials and Methods

In the following, the individual steps of the algorithm as shown in Figure 1 are discussed in detail. First, an initial ECG-gated reconstruction is performed. A thresholding operation removes non-vascular tissue. Then, a forward projection (FwP) is generated. The original projections are pre-processed by automatic top-hat filtering and thresholding. The FwP is then registered to the pre-processed original projection data using

a deformable 2-D–2-D registration algorithm. The resulting 2-D motion field is compensated for during the backprojection step of a subsequent ECG-gated reconstruction. The procedure may be repeated for additional refinement. In Section II-H, the experimental setup used for the evaluation is presented.

A. Initial Reconstruction

An initial ECG-gated reconstruction is performed by inserting a weighting function λ into a standard FDK-type algorithm [8], [9]. Let $h_r \in [0,1]$ be the heart phase at which reconstruction shall be carried out. The ECG-gated FDK reconstruction $f_{h_r} : \mathbb{R}^3 \mapsto \mathbb{R}$ at a voxel $\boldsymbol{x} \in \mathbb{R}^3$ is given by

$$f_{h_r}(\boldsymbol{x}) = \sum_{i=1}^{N} \lambda(i, h_r) \cdot w(i, \boldsymbol{x}) \cdot p_F(i, A(i, \boldsymbol{x})) , \quad (1)$$

where N is the number of projection images, $w : \mathbb{N} \times \mathbb{R}^3 \mapsto \mathbb{R}$ is the FDK distance weight and $p_F(i, \boldsymbol{u}) : \mathbb{N} \times \mathbb{R}^2 \mapsto \mathbb{R}$ is the filtered and redundancy-weighted projection data of the i-th image at pixel position $\boldsymbol{u}$. The pixel position is determined by the perspective projection of voxel $\boldsymbol{x}$, $A : \mathbb{N} \times \mathbb{R}^3 \mapsto \mathbb{R}^2, (i, \boldsymbol{x}) \mapsto A(i, \boldsymbol{x}) = \boldsymbol{u}$. The weighting function λ is a cosine-window defined by

$$\lambda(i, h_r) = \begin{cases} \cos^a\left(\frac{d(h(i), h_r)}{\omega}\pi\right) & \text{if } d(h(i), h_r) \leq \frac{\omega}{2} \\ 0 & \text{otherwise} \end{cases}, \quad (2)$$

where $h(i)$ is the heart phase of the i-th projection image according to the ECG, $\omega \in [0,1]$ controls the width and $a \geq 0$ controls the shape of the gating window. The distance measure d is defined as $d(h_1, h_2) = \min_{j \in \{0,1,-1\}} |h_1 - h_2 + j|$.

Additionally, a streak reduction [9] is performed to reduce undersampling artefacts.

B. Thresholding and Forward Projection

Since the contrasted cardiac vasculature presents a high-contrast object, a simple thresholding operation can be used to remove background structure. It retains only the $t_r \in [0,1]$ percentile of the largest voxel values. Then, maximum intensity forward projections p_{fwp} are generated from the thresholded initial reconstruction using the original acquisition geometry.

C. Pre-Processing of Original Projections

A background reduction is performed on the original projection data. First, a morphological top-hat filtering using a kernel of radius r as in [10], then a thresholding that retains only the $t_p \in [0,1]$ percentile of the largest pixel values is done. This removes most of the non-vascular background while safely retaining vascular structure. The processed projection images are denoted p_{bgr} in the following.

D. Registration Method

Registration establishes a mapping between the space of the pre-processed projection data p_{bgr} and the FwP p_{fwp} so that $p_{\text{bgr}}(i, \boldsymbol{u})$ is similar to $p_{\text{fwp}}(i, M(i, \boldsymbol{u}))$, where $M : \mathbb{N} \times \mathbb{R}^2 \mapsto \mathbb{R}^2$ is the motion vector field for the i-th image. We chose a uniform cubic B-spline as a deformable motion model

[11]. The mapping is parametrised by the number of B-spline control points c in each dimension. This model is very flexible, while containing an implicit smoothness constraint that avoids large local deformations for small values of c.

Mutual information [12] was used as a (multi-modality) similarity metric for the registration process. Mono-modal metrics like sum of squared differences cannot be used, since the grey values of p_{bgr} and p_{fwp} differ due to the maximum intensity FwP and data truncation. A gradient descent method was used to drive the registration process.

E. Motion Compensated Reconstruction

Using the motion vector field M, the estimated motion can be compensated for in the reconstruction step

$$f_{h_r, M}(\boldsymbol{x}) = \sum_{i=1}^{N} \lambda(i, h_r) \cdot w(i, \boldsymbol{x}) \cdot p_F(i, M(i, A(i, \boldsymbol{x}))). \quad (3)$$

Motion compensation applies a 2-D deformation after the perspective projection instead of a 3-D deformation before the projection [8].

F. Further Iterations

The process can be repeated for an additional refinement of the motion compensation by using the output from Step II-E as input in Step II-B.

G. Considerations on Implementation

The main contribution to processing time is by the registration process. Since registration is performed on a per-image basis, the projection stack can be processed in parallel. In addition, only those images need to be considered that have a gating weight $\lambda > 0$. Using graphics hardware is work in process. An optimal parameter set for the mutual information calculation can be found using the methods presented in [13]. Backprojection can be implemented very efficiently on graphics hardware [14], as can be B-spline evaluation [15]. Therefore, the motion compensated backprojection can be carried out completely parallelised on the graphics card.

H. Experimental Setup

For evaluation, two clinical datasets were used, where a left (LCA) or a right (RCA) coronary artery was contrasted respectively. Patient heart rates were 103 ± 7.0 bpm (LCA) and 68 ± 1.5 bpm (RCA). All datasets were acquired using a five second rotational angiography with selective contrast agent administration (1-2 ml/s). Source-isocentre-distance was ~80 cm and source-detector-distance ~120 cm. The acquired 133 projection images per dataset had a size of 1240x960 pixels with a pixel size of 0.308 mm. The size of the 3-D volumes after reconstruction was 256x256 voxels with 224 (LCA) and 186 (RCA) slices and an isotropic voxel size of 0.48 (LCA) and 0.60 (RCA) mm.

The gating parameters were selected as $\omega = 0.4$ and $a = 4$, with $h_r = 0.47$ (LCA) and $h_r = 0.75$ (RCA). Therefore, 52 projection images were used for reconstruction of each dataset after gating. Thresholding was performed at $t_r = 0.005$

Table I: Estimated noise in HU around coronary tree.

Name	Initial	One Iter.	Two Iter.
LCA	12.02	11.71	10.65
RCA	25.55	21.97	21.80

and $t_p = 0.2$. The size of the morphological kernel was $r = 3.4\,\mathrm{mm}$. The number of B-spline control points was set to $c = 5$ in each dimension. Two iterations of the algorithm were performed.

I. Evaluation

Qualitative evaluation was carried out visually. For a quantitative evaluation, image noise in the region of the reconstructed vessels was estimated [16] (on a sub-volume of $653\,\mathrm{cm}^3$ (LCA) and $387\,\mathrm{cm}^3$ (RCA) respectively). Additionally, vessel sharpness [17] was calculated for five different segments (cf. Figures 3a, 3d) along the coronary tree. To this end, one continuous branch of each tree was selected and 40 regularly spaced measurement sites were placed along each branch. At every site, 10 cross-sectional profiles equally distributed over $180°$ in the plane perpendicular to the vessel were used for the sharpness estimation. The values presented in Figures 3c and 3f are the average values of all sharpness measurements in the respective segments.

III. Results and Discussion

Figure 2 shows an original and a pre-processed projection, and a chequerboard overlay of a pre-processed projection with a FwP before and after registration for dataset LCA. The displacement of vessel sections in the FwP compared to the original projection is significantly reduced by the registration step. In Figure 3, the resulting reconstructions both before and after two iterations of the proposed algorithm are shown. It can be seen that the artefact level is strongly decreased, while the visibility and sharpness of structure is increased when using our proposed algorithm. This observation is confirmed both by a decrease of image noise (cf. Table I) and an increase in vessel sharpness (cf. Figure 3c and 3f) after registration. The second iteration step increases image quality and vessel sharpness for most segments.

IV. Conclusion and Outlook

Due to non-ideal gating, residual motion corrupts ECG-gated cardiac reconstructions. We presented an algorithm that compensates residual motion. Motion is estimated by a deformable 2-D–2-D registration method. No explicit segmentation is needed for registration. Motion is directly compensated for in the backprojection step of image reconstruction. The method can be repeated in an iterative loop.

We showed that artefact level is greatly decreased, while sharpness and detail of structure is increased.

References

[1] H. Hetterich, T. Redel, G. Lauritsch, C. Rohkohl, and J. Rieber, "New X-ray imaging modalities and their integration with intravascular imaging and interventions," *The International Journal of Cardiovascular Imaging (formerly Cardiac Imaging)*, vol. 26, no. 7, pp. 797–808, 2010.

[2] K.-J. Gutleben, G. Nölker, G. Ritscher, H. Rittger, C. Rohkohl, G. Lauritsch, J. Brachmann, and A. M. Sina, "Three-dimensional coronary sinus reconstruction-guided left ventricular lead implantation based on intraprocedural rotational angiography: a novel imaging modality in cardiac resynchronisation device implantation," *Europace*, vol. 13, no. 5, pp. 675–682, February 2011.

[3] B. Desjardins and E. Kazerooni, "ECG-gated cardiac CT," *American Journal of Roentgenology*, vol. 182, no. 4, pp. 993–1010, Apr. 2004.

[4] B. Perrenot, R. Vaillant, R. Prost, G. Finet, P. Douek, and F. Peyrin, "Motion correction for coronary stent reconstruction from rotational X-ray projection sequences," *IEEE Transactions on Medical Imaging*, vol. 26, no. 10, pp. 1412–1423, Oct. 2007.

[5] A. Lebois, R. Florent, and V. Auvray, "Geometry-constrained coronary arteries motion estimation from 2D angiograms – Application to injection side recognition," in *IEEE International Symposium on Biomedical Imaging: From Nano to Macro (ISBI)*, X. L. M. Wright, Steve; Pan, Ed. Chicago, IL, USA: IEEE, Mar. 2011, pp. 541–544.

[6] E. Hansis, D. Schäfer, O. Dössel, and M. Grass, "Projection-based motion compensation for gated coronary artery reconstruction from rotational x-ray angiograms," *Physics in Medicine and Biology*, vol. 53, no. 14, pp. 3807–3820, 2008.

[7] U. Jandt, D. Schäfer, M. Grass, and V. Rasche, "Automatic generation of time resolved motion vector fields of coronary arteries and 4D surface extraction using rotational x-ray angiography," *Physics in Medicine and Biology*, vol. 54, no. 1, pp. 45–64, Jan. 2009.

[8] D. Schäfer, J. Borgert, V. Rasche, and M. Grass, "Motion-compensated and gated cone beam filtered back-projection for 3-D rotational X-ray angiography," *IEEE Transactions on Medical Imaging*, vol. 25, no. 7, pp. 898–906, Jul. 2006.

[9] C. Rohkohl, G. Lauritsch, A. Nöttling, M. Prümmer, and J. Hornegger, "C-Arm CT: Reconstruction of Dynamic High Contrast Objects Applied to the Coronary Sinus," in *IEEE Nuclear Science Symposium and Medical Imaging Conference Record*, Dresden, Germany, Oct. 2008, pp. M10–328.

[10] E. Hansis, D. Schafer, O. Dossel, and M. Grass, "Evaluation of iterative sparse object reconstruction from few projections for 3-D rotational coronary angiography," *IEEE Transactions on Medical Imaging*, vol. 27, no. 11, pp. 1548–1555, Nov. 2008.

[11] M. Unser, "Splines: A Perfect Fit for Signal and Image Processing," *IEEE Signal Processing Magazine*, vol. 16, no. 6, pp. 22–38, Nov. 1999.

[12] D. Mattes, D. R. Haynor, H. Vesselle, T. K. Lewellyn, and W. Eubank, "Nonrigid multimodality image registration," in *Proceedings of SPIE*, M. Sonka and K. M. Hanson, Eds., vol. 4322, no. 1. San Diego, CA, USA: SPIE, Feb. 2001, pp. 1609–1620.

[13] D. Hahn, V. Daum, and J. Hornegger, "Automatic Parameter Selection for Multi-Modal Image Registration," *IEEE Transactions on Medical Imaging*, vol. 29, no. 5, pp. 1140–1155, May 2010.

[14] H. G. Hofmann, B. Keck, C. Rohkohl, and J. Hornegger, "Comparing performance of many-core CPUs and GPUs for static and motion compensated reconstruction of C-arm CT data," *Medical Physics*, vol. 38, no. 1, pp. 468–473, 2011.

[15] D. Ruijters, B. ter Haar Romeny, and P. Suetens, "Efficient GPU-Based Texture Interpolation using Uniform B-Splines," *Journal of Graphics, GPU, & Game Tools*, vol. 13, no. 4, pp. 61–69, 2008.

[16] S.-M. Yang and S.-C. Tai, "Fast and reliable image-noise estimation using a hybrid approach," *Journal of Electronic Imaging*, vol. 19, no. 3, pp. 033 007–1–15, July–September 2010.

[17] D. Li, J. Carr, S. Shea, J. Zheng, V. Deshpande, P. Wielopolski, and J. Finn, "Coronary Arteries: Magnetization-prepared Contrast-enhanced Threedimensional Volume-targeted Breath-hold MR Angiography," *Radiology*, vol. 219, no. 1, pp. 270–277, April 2001.

(a) Original Projection   (b) Pre-processed Projection   (c) Unregistered FwP   (d) Registered FwP
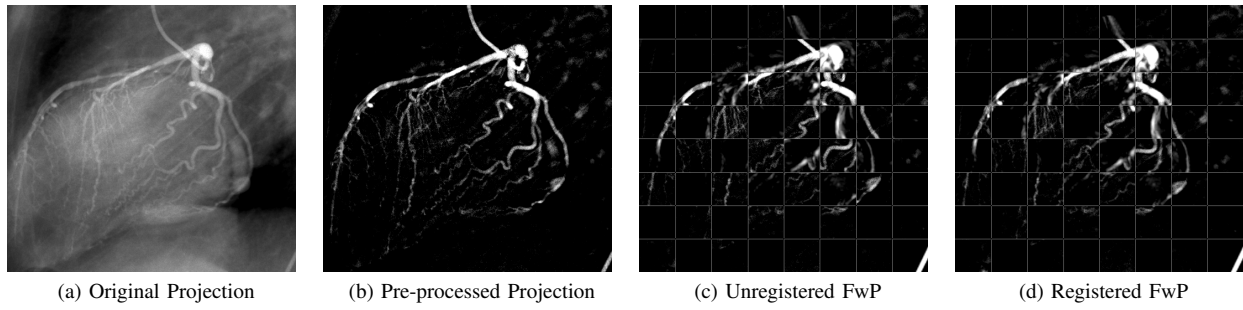
Figure 2: Results of the registration algorithm for dataset LCA.
In Figures 2c and 2d, the pre-processed projection and the FwP are shown combined in a chequerboard pattern to visualise the registration result.

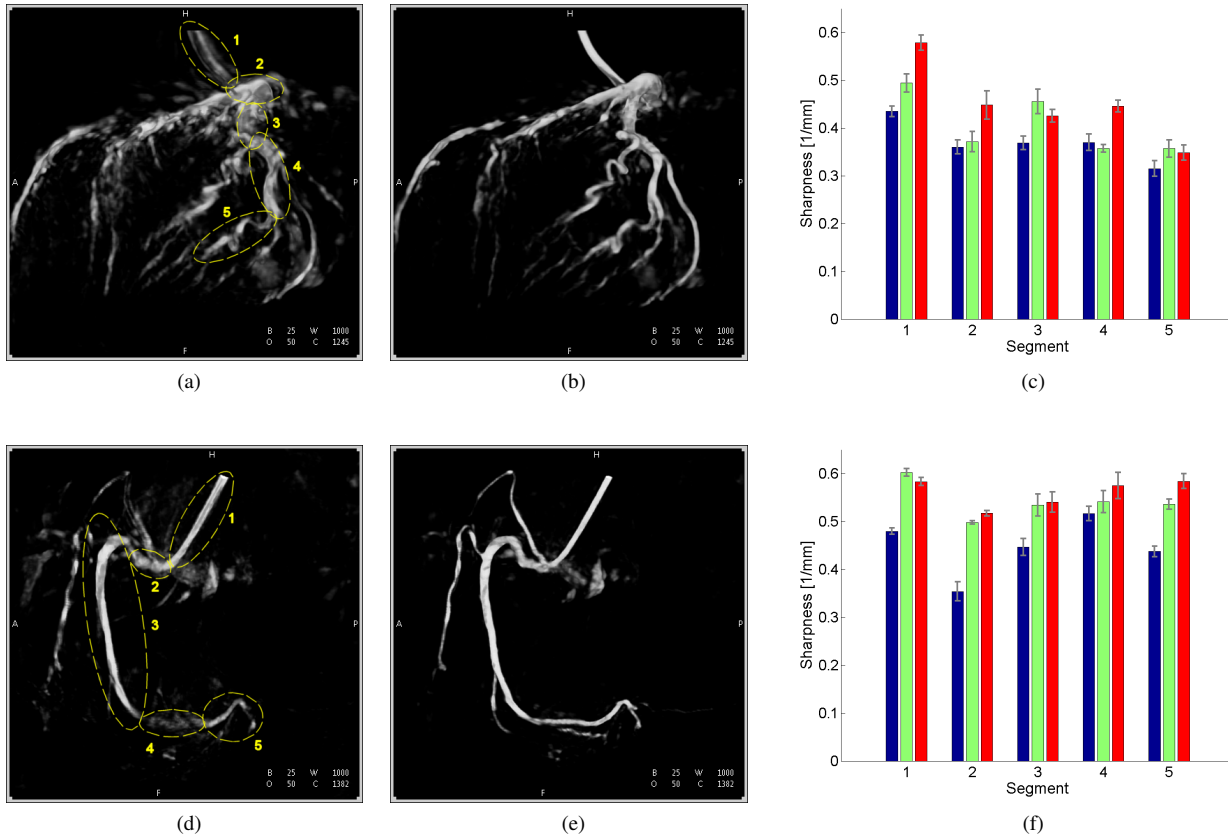

(a)   (b)   (c)

(d)   (e)   (f)

Figure 3: Reconstruction results without and after two iterations of the proposed algorithm.
Top row: LCA, bottom row: RCA. Left column: initial reconstruction (and segments for vessel sharpness measurements), middle column: compensated reconstruction, right column: vessel sharpness.
All volume renderings show a left sagittal view. The grey scale window was 1000. In the right column, the average vessel sharpness and standard deviation of the initial reconstruction (■), after one iteration (■) and after two iterations (■) are shown for each segment.